Science of the Total Environment 628–629 (2018) 291–301

Contents lists available at ScienceDirect

Science of the Total Environment

journal homepage: www.elsevier.com/locate/scitotenv

Recovery of black-necked swans, macrophytes and water quality in a Ramsar wetland of southern Chile: Assessing resilience following sudden anthropogenic disturbances

Eduardo Jaramillo [a,*], Nelson A. Lagos [b], Fabio A. Labra [b], Enrique Paredes [c], Emilio Acuña [a], Daniel Melnick [a], Mario Manzano [a], Carlos Velásquez [a], Cristian Duarte [d]

[a] Instituto de Ciencias de la Tierra, Facultad de Ciencias, Universidad Austral de Chile, Valdivia, Chile
[b] Centro de Investigación e Innovación para el Cambio Climático, Facultad de Ciencias, Universidad Santo Tomás, Santiago, Chile
[c] Instituto de Patología Animal, Facultad de Ciencias Veterinarias, Universidad Austral de Chile, Valdivia, Chile
[d] Departamento de Ecología y Biodiversidad, Facultad de Ecología y Recursos Naturales, Universidad Andrés Bello, Santiago, Chile

HIGHLIGHTS

- In 2004, the Rio Cruces wetland, a Chilean Ramsar site was affected by an anthropogenic disturbance.
- Swan numbers and weights decreased drastically across the wetland.
- Swan decrease correlated with abundance of their main food source: the macrophyte *Egeria densa*
- Swan hepatic abnormalities were associated with increased iron content in *E. densa*.
- The swan population and *E. densa* cover returned to normal conditions in 8 years.

GRAPHICAL ABSTRACT

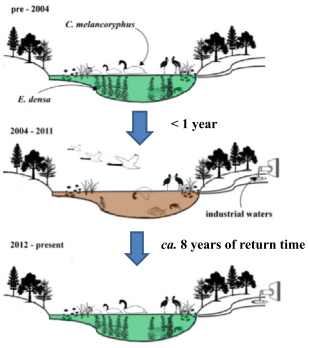

ARTICLE INFO

Article history:
Received 3 October 2017
Received in revised form 31 January 2018
Accepted 31 January 2018
Available online xxxx

Editor: Daniel Wunderlin

Keywords:
Wetlands
Ramsar site
Southern Chile
Herbivorous water birds
Aquatic macrophytes
Industrial waters

ABSTRACT

In 2004 migration and mortality for unknown reasons of the herbivorous Black necked swan (*Cygnus melancorhyphus* (Molina, 1782)) occurred within the Río Cruces wetland (southern Chile), a Ramsar Site and nature sanctuary. Before 2004, this wetland hosted the largest breeding population of this water bird in the Neotropic Realm. The concurrent decrease in the spatial occurrence of the aquatic plant *Egeria densa* Planch. 1849 - the main food source of swans - was proposed as a cause for swan migration and mortality. Additionally, post-mortem analyses carried out on swans during 2004 showed diminished body weight, high iron loads and histopathological abnormalities in their livers, suggesting iron storage disease. Various hypotheses were postulated to describe those changes; the most plausible related to variations in water quality after a pulp mill located upstream the wetland started to operate in February 2004. Those changes cascaded throughout the stands of *E. densa* whose remnants had high iron contents in their tissues. Here we present results of a long-term monitoring program of the wetland components, which show that swan population abundance, body weights and histological liver conditions recovered to pre-disturbance levels in 2012. The recovery of *E. densa* and iron content in plants throughout the wetland, also returned to pre-disturbance levels in the same 8-year time period. These results show the temporal scale over which resilience and natural restoring processes occur in wetland ecosystems of temperate regions such as southern Chile.

* Corresponding author.
E-mail address: ejaramillo@uach.cl (E. Jaramillo).

https://doi.org/10.1016/j.scitotenv.2018.01.333
0048-9697/

1. Introduction

Wetlands are areas of marsh, fen, peat land, swamps, wooded wetlands, whether natural or artificial, permanent or temporary, with water that is static or flowing, which may be fresh, brackish or salty, including coastal areas of marine water to a depth which at low tide it does not exceed six meters (www.ramsar.org). Wetlands provide valued ecosystem services to society, including water purification, carbon storage, trapping of nutrients and pollutants, sediment and flood control, biodiversity maintenance, fisheries and tourism, among others (e.g., Zedler and Kercher, 2005). In spite of their importance, wetlands are frequently degraded by human-induced activities such as land conversion to agriculture, water extraction and overloads of polluted waters (e.g., Zedler and Kercher, 2005).

Due the broad degradation of wetland ecosystems, many efforts have been attempted for their restoration, with different level of success, highlighting the importance of integrating resilience in restoration planning, The latter is now envisioned as a dynamic and adaptive process, in which natural variability has paramount importance in reducing risk of population decline and loss of ecosystem services; for instance, when confronting uncertain climate impacts (e.g., Timpane-Padgham et al., 2017). Therefore, identifying the spatial and temporal scales of natural variability in ecosystems will improve decision -taking processes in restoration objectives operating at different biodiversity levels (i.e. individuals, population, and communities; e.g. Naeem and Li, 1997). Resilience describes the capacity of an ecosystem to absorb disturbances, as it reorganizes and retains their dynamical structure through mechanisms such as resistance to and recovery from perturbations (e.g. Walker et al., 2004). Thus, understanding recovery timescales of wetland ecosystem components after a natural or anthropogenic disturbance, provide a unique opportunity to estimate resilience in a broad perspective (Ives, 1995; Neubert and Caswell, 1997).

To date, nearly 14 million hectares in 1600 sites around the world have been designated as wetlands of international importance; thirteen of these sites are in Chile (spanning nearly 362.000 ha) (http://www.ramsar.org). Until 2004, the Río Cruces wetland, a Ramsar Site and a nature sanctuary adjacent to the city of Valdivia (40°S), was the main breeding site of the charismatic herbivorous Black-necked swan, *Cygnus melancorhyphus* (Molina, 1782) (swans hereafter) in the Neotropic Realm (Schlatter, 1998; Schlatter et al., 2002). This swan is an herbivorous water bird (Corti and Schlatter, 2002) and the only native species of the genus *Cygnus* in this biogeographic region (Araya and Millie, 1986; Navas, 1977). Its geographic distribution spans southern Brasil, Paraguay, Uruguay, Argentina and much of Chile (Casares, 1933; Schlatter et al., 1991a, 1991b). Data collected from 1986 to 2004 showed that the breeding season of this swan extended from June to September, with a mean clutch size (all seasons included) close to 3.1 eggs (Silva et al., 2012). The swan population at the Río Cruces wetland consisted of ~12,000–14,000 swans in 1994–1996, likely well above carrying capacity. Between 2000 and 2004, the population declined to around 5000–6000 birds (data from Corporación Nacional Forestal (CONAF), Chile; www.conaf.cl). At that time, these water birds were primarily supported by *Egeria densa* Planch. 1849 (Corti and Schlatter, 2002), an aquatic macrophyte which used to be the dominant submerged plant in the wetland (Steubing et al., 1980).

However, the swan population of the Río Cruces wetland decreased primarily due to emigration starting in mid-2004, with only a couple of hundred individuals observed during 2005–2006 (Lagos et al., 2008). This emigration event resulted in higher abundances in wetlands away from Río Cruces. For example, Ramírez et al. (2006) reported increases in swan abundance after 2004 at the Lago Lanalhue and the urban lagoons in the city of Concepción (200 and 320 km north of the Río Cruces wetland, respectively). This emigration event was clearly not related to major environmental process that operates at interannual timescales such as ENSO events (Schlatter et al., 2002). In addition to population decreases due to emigration, absence of nest and chicks and mortality of swans due to previously-unknown causes were observed (Jaramillo et al., 2007; www.conaf.cl). For example, nearly 100 dead swans were found during 2004–2005 in the wetland. Concurrently, a reduction in the spatial occurrence of *E. densa* was also observed and water turbidity changed notoriously due to a higher load of suspended solids, a fact inferred to be caused by the demise of the natural anchor of sediments by the formerly abundant *E. densa* (Lagos et al., 2008). The macrophyte *E. densa* plays a crucial role in determining the degree of food availability for herbivorous water birds (Corti and Schlatter, 2002), the functional group that presented stronger impacts across the wetland as compared with carnivorous birds (Lagos et al., 2008).

During the spring of 2004, the former National Environmental Commission of Chile (CONAMA) commissioned a study to the Universidad Austral de Chile (UACh hereafter), to primarily assess the causes of swan emigration and mortality. Post-mortem analyses showed emaciation, high concentrations of iron and histopathological abnormalities in their livers. In addition, necrotic patches and higher loads of heavy metals (mainly iron) in remaining *E. densa* plants collected within the wetland as compared with healthy plants collected outside this area, were also observed (UACh, 2005). The most plausible hypothesis, stated that these situations were associated with significant changes in water quality within the wetland, concomitant with the onset in early 2004 of a new wood pulp mill located 25 km upstream from the wetland (Escaida et al., 2014). Those changes would have originated in a sudden short-lived spillage of residual waters from the pulp mill that resulted in high concentrations of some chemicals in the wetland waters, a fact subsequently detected by monitoring programs (UACh, 2014). The abrupt decrease of *E. densa* was concomitant with those changes in water quality resulting in the emaciation of swans. In addition, histopathological abnormalities in the livers of dead swans were associated with high iron contents in remaining *E. densa* plants (Jaramillo et al., 2017; submitted). Those results strongly suggest that the wetland was subjected to the cascading impacts of a disturbance event (Pinochet et al., 2004; UACh, 2005; Woelfl et al., 2006; Jaramillo et al., 2007; Lagos et al., 2008; Escaida et al., 2014). A legal procedure was initiated during 2005 by the State Defense Council of Chile and in July 2013, the Civil Court of Valdivia ruled that the wood pulp mill was responsible for the environmental changes described above, supporting conclusions of an earlier study (UACh, 2005). Consequently, the Civil Court of Valdivia ordered a series of measures to mitigate the damage to the wetland, including evaluation and monitoring programs. The results showed that after 2006, concentrations of chemicals in wetland waters are below thresholds specified by Chilean environmental regulations (UACh, 2014, 2015, 2017).

Since 2004, we have monitored the Río Cruces wetland quantifying swan population abundances and spatial occurrence of *E. densa*. In this study, we assess the resilience of these two ecosystem components, as well as the current environmental state of the Río Cruces wetland and its tributary rivers (the wetland hereafter). We evaluated the temporal variability of the main ecosystem components altered in 2004: i) swan population abundances, ii) body weights, histopathological conditions and iron concentrations of hepatic tissues of swans, iii) spatio-temporal variability of *E. densa* and iv) water quality within and outside the wetland.

2. Material and methods

2.1. Study area

The Río Cruces wetland (Fig. 1) includes a nature sanctuary under Chilean law and the first Neotropical Wetland of International Importance by the Ramsar Convention, both established in 1981. The sanctuary (4877 ha) and shallow water zones of the tributary rivers of Río Cruces (i.e. the wetland), originated during May 1960 as a result of land subsidence caused by the 1960 earthquake, the largest seismic

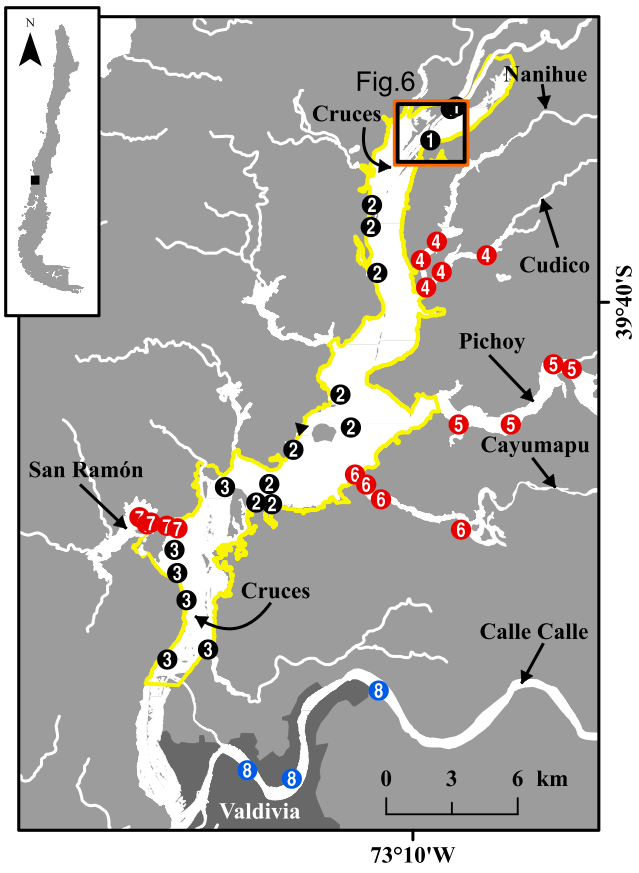

Fig. 1. Location of the Río Cruces wetland and its tributaries, north of the city of Valdivia, southern Chile. The yellow line encloses the Ramsar Site and nature sanctuary. Numbers denote sites visited to study the spatial occurrence of *Egeria densa* between 2008 and 2016: black dots indicate sites within the Ramsar area, while red and blue dots are for sites within the tributaries and outside the wetland, respectively. Number of sites refers to the eight sectors studied across the Ramsar area, the tributaries and Río Calle Calle. The orange-framed rectangle shows extent of the 2016 drone flight.

event recorded by modern seismology with a moment magnitude of 9.5° (e.g., Plafker and Savage, 1970; Cisternas et al., 2005). The importance of this area for swan reproduction, as well as the high diversity of water birds and aquatic plants (Ramírez et al., 1991; San Martín et al., 2000), among other reasons justified its inclusion to the Ramsar Convention.

2.2. Population abundances of swans

Monthly surveys carried out by Corporación Nacional Forestal (CONAF, Chile; www.conaf.cl) between January 1987 and December 2016, were used to analyze intra and inter-annual trends in population abundances of swans. The sampling protocol included two approaches: fixed censuses at 16 sites distributed across the central wetland and its tributary rivers, and mobile censuses to count birds usually hidden. Both censuses were carried out during two full days.

Intra and inter-annual trends in abundance were analyzed using LOWESS (Locally Weighted Scatterplot Smoothing; cf. Lagos et al., 2008). The corresponding trend was explored using the f-factor (o tension) (i.e. the proportion of adjacent data-points used to estimate the predicted value at the focal point) and selecting those resulting in normal residuals for the fitted trend (Trexel and Travis, 1993). In general, an *f*-factor of 0.2 and 0.4 was selected for inter and intra-annual trends, which yield significant fits to the corresponding data (inter-annual: $r^2 = 0.76$; intra-annual: $r^2 = 0.98$; $p < 0.001$ in both cases). ANOVA with Tukey test as a posteriori comparison between pairs of consecutive years was performed to assess inter-annual differences in swan abundances (Zar, 1999). Abundance data were $\log_{10}$ transformed and no strong deviation from ANOVA assumptions was observed in assessing normality of residuals using Kolmogorov test and homoscedasticity using F-Max test. All these analyses were done using General Linear Models procedure implemented in MINITAB v14 software (Minitab Inc., Pennsylvania, USA).

2.3. Post mortem analyses of swans and data analyses

We carried out necropsies in swans to explore their body condition and causes of mortality. 40 swans were collected from the study area during October 2004–January 2005; 16 of those birds were dead and 24 moribund. Necropsies involved body weight measurements and protocols for post mortem examination, including histopathology of liver. The tissues were embedded on paraffin sections cut at 5 μm intervals and stained with hematoxylin and eosin (H&E) and Prussian blue stain (sensitive to iron). Sections of liver from 36 swans were stored (−20 °C) for later iron content analysis by Flame Atomic Absorption Spectrometry (FAAS) following the method of Miller-Ihli (1990). Pigmentation and histopathological alterations of hepatic tissues were qualitatively graded on a 0–3 scale (cf. Farina et al., 2005). Due to the presence of zero's and low frequencies, the grades of histopathological alterations in livers of swans (counts) collected in the wetland during 2004–2005 and 2012 (see below) were compared using two-tail Fisher's exact test for a 2×4 contingency table.

Swan body weights, histopathological and iron content of liver data from 2004 to 2005 were compared with equivalent data collected during 2002, 2003 (Verdugo, 2004), 2012, 2014, 2015 and 2016 (see Table 1). To examine changes in body weight distribution, we compared the nonparametric probability density estimates across different years. Body weight probability density distributions, were estimated in the R environment using the KernSmooth package (Wand and Jones, 1995; Wand and Ripley, 2015). Since distribution of iron data was not normal (Sokal and Rohlf, 1995; Zar, 1999), we used the non-parametric Kruskal-Wallis test. Similarities and inter-annual differences in mean iron contents were then compared with the a posteriori multiple comparison Fisher's LSD test (Fisher, 1935; Saville, 1990).

2.4. Field surveys and remote sensing analyses of the spatial occurrence of E. densa

Between 2008 and 2016, we visited 36 sites to evaluate the inter-annual variability of the spatial occurrence of *E. densa*, concentration of total suspended solids (TSS) and water transparency in the wetland (Fig. 1); these visits were carried out during low river flow periods (late March & early April). We also examined four sites along Calle Calle river adjacent to the wetland (Fig. 1) and considered as control sites because here the spatial occurrence of *E. densa* has not changed since 2004. The occurrence of *E. densa* was measured as the percentage of sites with presence of plants. Water samples were collected with 1 L plastic bottles at an approximate depth of 20 cm; these samples were filtered through glass fiber filters of 5 cm diameter and pore size of

Table 1
Sampling seasons and number of swans examined to compare body weights and number of analyses (i.e. swans) carried out to evaluate histopathological conditions and iron contents of swan's livers in the study area.

Sampling periods	Body weight	Histopatological conditions	Iron contents
Spring 2002			2
Winter 2003	51		
Spring & summer 2004–2005	40	40	36
Summer & autumn 2012	42	13	12
Winter 2014			4
Summer 2015	30		

0.48 μm. TSS was measured as the dry mass of particles retained on that filters after drying it in an oven at 60 °C for 24 h (Strickland and Parsons, 1972). Water transparency was measured with a Sechi disk (Lagos et al., 2008; Lee et al., 2016).

The temporal variability of *E. densa*'s across the wetland was described by fitting a logistic regression model to the proportion of cover as a function of sampling years in all eight zones studied (cf. Fig. 1). We used a logistic sigmoid model $y = a / (1 + \exp(-b * (x - c)))$, where *a* corresponds to the function's maximum value, *b* corresponds to the function's steepness or maximum rate of increase, and *c* corresponds to the temporal location of the curve's midpoint. All these three parameters were estimated from the data using procedure *nls* in the R program. We also fitted a linear model, using procedure *lm* in the stats library in the R program (Crawley, 2013; R Development Core Team, 2014). Both the logistic and linear regression models were ranked according to the Bayesian information criterion (BIC or Schwarz criterion; Schwarz, 1978). Once fitted, the model with the minimum BIC was selected (Schwarz, 1978). On the other hand, visual inspection of both TSS and water transparency data across the eight study zones revealed absence of sigmoid trends. Hence, temporal variation in both TSS and water transparency data across all eight study zones were described using linear models, implemented in the R program (R Development Core Team, 2014).

To estimate a Habitat Suitability Index (HSI), we fit an ecological niche model to the *E. densa* data. Thus, Maximum Entropy Species Distribution Modelling software v.3.3 (MaxEnt) was used. This software uses information on spatial occurrences and GIS layers or features to calculate a probability function that describes the chances of observing a presence across the study area (Phillips et al., 2004, 2006; Phillips and Dudík, 2008; Elith et al., 2011). Several studies have shown that this method performs better in relation to similar ones (e.g. Elith et al., 2006; Ortega-Huerta and Peterson, 2008), being particularly effective even in situations where the sample size is small (Pearson et al., 2007; Papes and Gaubert, 2007; Wisz et al., 2008). It has been pointed out that fitting maximum entropy model is equivalent to maximizing the likelihood function of a spatial inhomogeneous Poisson point process (Aarts et al., 2012; Fithian and Hastie, 2013; Renner and Warton, 2013). Hence, its output can be interpreted as providing relative density estimates across space (Aarts et al., 2012; Renner and Warton, 2013), providing a measure of environmental habitat suitability (HSI) for the species under study.

To obtain geo-referenced occurrences of pure stands of this plant, field sampling was conducted during the spring-summer season of 2014–2015, recording large dominant or mono specific patches of *E. densa* (30 m diameter or larger) The patch coordinates at the center were registered using a WSG84 coordinate system with a UTM datum (18S zone). These points of occurrences were used together with a set of remote sensing GIS layers. Remote sensing layers were extracted from a Landsat 8 operational land imager (OLI) image. The OLI image used was recorded on location 233/88 of the path/row of Worldwide

Reference System 2 (WRS-2). This WRS-2 path/row location is centered at 40°19′20″ S, 72°51′00″ W, and encompasses the entire wetland. The image used to describe the 2014–2015 summer season was captured on January 28, 2015 (see Supplementary Table S1). To extract the predictor GIS layers, bands 2 through 7 of the OLI image were processed following Lagos et al. (2008). Thus, each band was radio metrically calibrated using Landsat 8 radiance rescaling factors provided in the image metadata file, to calculate top of atmosphere spectral radiance values ($L\lambda, W \cdot (m^2 \cdot sr \cdot \mu m)^{-1}$). These Lλ values were then transformed to top-of-atmosphere reflectance percentages (R_{TOA}) (Chander and Markham, 2003), and further corrected by applying an atmospheric correction for Case-2 turbid waters, using the path extraction method (Ahn et al., 2004; Lagos et al., 2008). In addition, after calibration and processing, we calculated the blue/green ratio (Band 1/Band 2), as a proxy for chlorophyll content in the water. Also, bands 4 and 5 were used to estimate the normalized difference vegetation index (NDVI) and the enhanced vegetation index (EVI). NDVI was calculated (Masek et al., 2006) as: NDVI = (Band 5 − Band 4) / (Band 5 + Band 4), EVI = 2.5 × ((Band 5 − Band 4) / (Band 5 + 6 × Band 4–7.5 × Band 2 + 1)). Also, in order to identify open water sections corresponding to the rivers and wetland, the modified normalized water difference index (Xu, 2006) was calculated as: MNDWI = (Band 2 − Band 6) / (Band 2 + Band 6), where Band 2 and 6 correspond to green and short wave infrared or middle infrared radiation (Xu, 2006). This yielded a set of 10 GIS layers corresponding to 5 top-of-atmosphere reflectance percentages (Bands 2 through 7) and four indexes (NDVI, EVI, blue/green ratio and MNDWI).

Once processed, all 10 GIS layers were used to fit an ecological niche model for *E. densa* across the wetland. To fit the MaxEnt ENM for this macrophyte, we used a 6-fold cross-validation scheme, thus allowing every occurrence data point to be used as part of the training and evaluation data sets (Phillips et al., 2004, 2006; Phillips and Dudík, 2008; Elith et al., 2006; Elith et al., 2011). This yielded a spatially explicit estimation of HSI values for *E. densa* across the wetland in the 2014–2015 spring-summer season. To estimate historical variation in HSI values for *E. densa*, the MaxEnt model fitted on the 2014–2015 occurrences and remote sensing data was transferred or projected using remote sensing images from previous summer seasons to hind cast the spatial distribution of habitat suitability for *E. densa* in previous years. This corresponds to a retrospective projection based on the fitted ecological niche model (Elith and Leathwick, 2009). To this end, we used the model to predict expected HSI values across the wetland, using Landsat 5 thematic mapper (TM) remote sensing images for previous years. Specifically, TM images for WRS-2 location 233/88 were downloaded for the spring-summer seasons of 1999–2000, 2004–2005 and 2009–2010 (see Supplementary Table S1 for details on the Landsat images used). All these three TM images were processed in the same manner as described previously for the Landsat 8 OLI image, obtaining the same 10 layers for each of these temporal samples. These three sets of GIS layers were used together with the 2014–2015 fitted MaxEnt model to predict the expected HSI values across the wetland for those three spring-summer seasons (1999–2000, 2004–2005 and 2009–2010). This yielded a time series set of four spatially explicit estimates of HSI values across the wetland.

3. Results and discussion

3.1. Temporal variability in population abundances of swans

Swan abundance varied significantly among years (ANOVA: $F(29.356) = 64.87$: $p < 0.001$). The comparisons carried out between sequential pairs of years, indicate the occurrence of temporal milestones with significant changes in populations abundances between pair of years; in particular, between the years 1988–1989, 1993–1994, 2004–2005 and 2011–2012 (Tukey test, $p < 0.05$; asterisks in Fig. 2a).

These inter-annual changes in swan abundances were also associated with differences in the intra-annual fluctuations (colored bars in Fig. 2a). For instance, during 1987 and 1988, population abundances were relatively low and stable, but a significant increase in swan abundance was observed from 1989 to 1993, concomitant with regular cycling or intra-annual fluctuations (i.e. periods i and ii, Fig. 2b). A third period is recognizable from 1993 to 2004, associated with a sustained increase in swan abundance and large intra-annual fluctuations (i.e. period iii, Fig. 2b). The period 2004–2011 was characterized by an abrupt decrease to low and stable abundances at both inter as intra-annual scales (i.e. period iv, Fig. 2b). In 2012–2013, a significant increase in the abundance of swans indicated the start of a recovery period, with regular intra-annual fluctuations (i.e. period v, Fig. 2b). The population continued to recover during 2014–2016, with increased intra-annual fluctuations, and averaged annual abundances, similar to those occurring during the period 1994–2004.

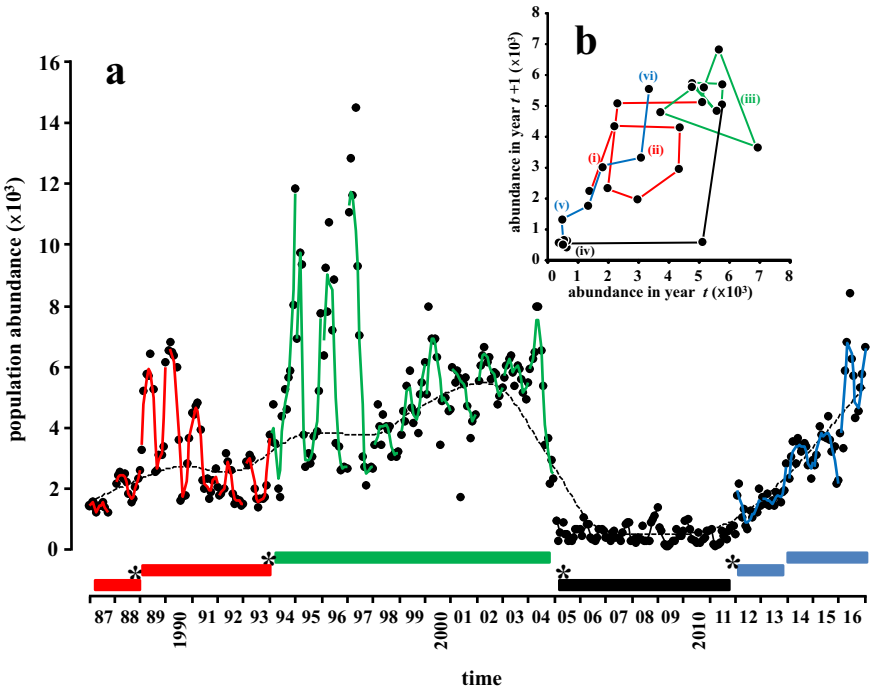

Fig. 2. a) Temporal fluctuations in population abundances of swans recorded in the Rio Cruces wetland from January 1987 to December 2016. Continuous and dashed lines correspond to intra and inter-annual trends fitted to the observed data. Significant differences in abundances between sequential pair of years are depicted by asterisks; the box aligned above the x-axis identify similar abundances across years. b) Pathways characterizing inter and intra annual fluctuations in abundances of the swans: (i) initial period with low and stable abundances (1987–1988, red line); (ii) period of increased abundances with regular intra annual fluctuations (1989–1993, red line); (iii) period of further increases in abundances with large intra-annual fluctuations (1994–2004, green line); (iv) decayment period to low and stable abundances (2005–2011, black line); (v) initial recovery period with small intra annual fluctuations (2011–2012, blue line); (vi) increased recovery with regular intra annual fluctuations (2013–2016, blue line). Similar color codification is used to identify these temporal periods (i to vi) in (a) and (b).

Variability in swan abundance at the intra-annual scale may result from seasonal reproduction and breeding. Those processes interplay with ecological factors such as productivity, habitat availability and weather (e.g. Schlatter et al., 1991a, 1991b; Frederick and Ogden, 2001; Lagos et al., 2008; Skagen and Adams, 2012). Inter-annual fluctuations in population abundance have been ascribed to changes in hydrologic conditions and water quality in the region (Lagos et al., 2008), as well as large-scale, periodic perturbations attributed to ENSO (El Niño Southern Oscillation) cycles which promote changes in distribution and colonization of wetlands across central and southern Chile (e.g. Vilina et al., 2002). These drivers of intra and inter-annual fluctuations may explain patterns recorded in the abundance of swans in the Río Cruces wetland. For instance, reduced mating and nesting success may explain low abundance during 1988 to 1993; increased variability observed from 1994 to 2004 may reflect increased success in breeding within years and fluctuations from year to year may reflect changes in habitat quality that influences productivity (Vilina et al., 2002). The long term-effects of the disturbance on water quality, and thus on breeding and colonization patterns are evident in the low and stable abundances recorded from 2004 to 2011 as showed by our previous studies (Jaramillo et al., 2007; Lagos et al., 2008); in contrast, for the recovery period, a gradually increasing inter and intra-variability reflect return to normal conditions and regular population dynamics. Similar patterns have been described for population dynamics of wetland birds showing strong temporal fluctuation in response to natural changes in ecological conditions in the Everglades (e.g., Frederick and Ogden, 2001; Frederick et al., 2009).

Only few examples of anthropogenic impacts on swan population abundances and on the return times have been studied. During the early 1900's, the trumpeter swan (*Cygnus buccinator* Richardson) was heavily impacted by the fur trade and by European settlement in north America, which reduced its numbers and distribution to only 69 birds registered in 1932, and breeding populations found only in Alaska until 1954 (Travsky and Beauvais, 2004). Following the conservation efforts in the 1960's, swan populations increased in abundance, but have not yet returned to their original size and distribution across North America (McIntyre, 2015). Studies on artificial wetland ecosystems indicate that the time scale required for avian communities to reach similar compositions to natural systems may take a decade or more (Snell-Rood and Cristol, 2003).

A recent study conducted between 2000 and 2010 suggested that both the dynamics and distribution of black-necked swan population showed distinctive patterns when comparing before and after the environmental changes occurring in 2004 (e.g. Gonzalez and Fariña, 2013). Similar results were previously reported by studies performed early after the abrupt environmental changes (e.g. Lagos et al., 2008). The temporal scales of these early and following studies do not allow the assessment of the recovery time of the black-necked swan population. Thus, although establishing protected areas may be effective, (e.g. Gonzalez and Fariña, 2013), they may be unnecessary given the observed ecosystem resilience as a buffer that protects the ecosystem from management actions based upon incomplete ecological understanding.

3.2. Body weight of swans, iron contents and histopathology of hepatic tissues

Changes in swan body weights throughout the study period are shown in Fig. 3a. In addition to the decrease in population abundance, the swans presented a sharp decrease in mean body weight during the spring and summer 2004–2005 as compared to the data collected previously (winter 2003). Body weights recovered by summer & autumn 2012 and presented a subsequent increase by the summer 2015 and throughout autumn 2016. Thus, body weight probability distributions (Fig. 3a) show that swan body condition has recovered

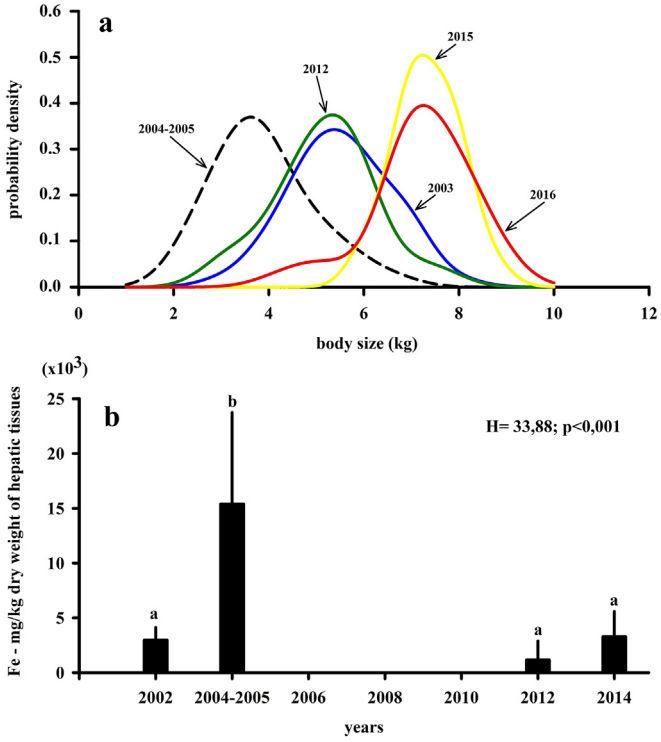

Fig. 3. a) Inter annual variability in the body weights of swans. The lines correspond to swans studied during winter 2003 (blue line), spring & summer 2004–2005 (dashed black line), summer & autumn 2012 (green line), summer 2015 (yellow line) and autumn 2016 (red line). b) Inter-annual variability in the iron contents of swan´s livers.

substantially after the observed decrease following the decrease of *E. densa* across the wetland during 2004.

Fig. 3b shows that the mean iron content in hepatic tissues of swans collected during the spring & summer 2004–2005, was significantly higher than mean iron contents estimated for swan's livers during 2002, 2012 and 2014 (Fig. 3b). Thus, the mean estimate for 2004–2005 (~15.430 Fe mg/kg dry weight of hepatic tissues) was nearly 4.7–13.3 times higher, than the mean values estimated for previous or post 2004–2005 data.

During *post-mortem* analyses we observed a coppery color of the liver of most swans and the following microscopic abnormalities of the hepatic tissue: hepatocytes strongly positives to Prussian blue stain, deposits of hemosiderin in the Kupfer cells, periportal inflammation, perivascular fibrosis, proliferation of bile ducts, nuclear enlargement, double nucleus and necrosis in some hepatocytes. Swans showed significant differences between 2004 and 2005 and 2012, in terms of grading of the liver histopathological abnormalities (χ^2; $p < 0.05$, Table 2). For the 2004–2005 period, there was higher occurrence of swans evidencing mild and severe liver alterations related to hepatocytes positives to Prussian blue stain (due to increased iron concentration), hemosiderin deposits in Kupfer cells, and periportal inflammation (Table 2 and Fig. S1). Although, for the 2012 period, these histopathological alterations still occurred in the swans, these were classified as slight or mild grading, with severe alterations occurring only in one of the analyzed birds.

Since hepatocytes of many of the dead swans examined during 2004–2005 showed severe positive staining to Prussian blue stain (an iron specific stain) and that iron contents of hepatic tissues of these swans were significantly higher, we concluded that this situation was compatible with iron storage disease associated with histopathological alterations - technically known as hemochromatosis (cf. Lowenstine and Munson, 1999; Klopfleisch and Olias, 2012; Lowenstine and Stasiak, 2015). This pathological situation has been documented for birds in captivity (Mynah birds, birds of paradise, toucans and tanagers) and is related to the high iron content of the offered food (Gosselin and Kramer, 1983; Kincaid and Stoskopf, 1987; Ward et al., 1988; Cork, 2000; Mete et al., 2001, 2003; Klasing et al., 2012), which may cause toxic effects, including fibrosis and cirrhosis in parenchymal organs such as the liver (cf. Lowenstine and Munson, 1999; Mete et al., 2003). Although the original definition of hemochromatosis corresponds to a hereditary disease in humans, where the high absorption of iron occurs in the intestine (Mete et al., 2003; Farina et al., 2005; Klopfleisch and Olias, 2012), the case studied here likely corresponds to a secondary hemochromatosis due to the consumption of iron-enriched *E. densa* plants. Iron content in plants collected during 2004–2005 within the wetland had significantly higher, ~4-fold, concentrations of iron than plants collected from outside the wetland (~30,000 vs. 8300 mg Fe/kg dry weight of plants; Jaramillo et al., 2017; Jaramillo et al., 2018; in review); consequently, the 3.6-fold increase of iron concentration measured in *E. densa* from within the wetland would explain the higher iron content in swan's livers collected from the wetland area during 2004–2005, as compared with samples collected from swans studied during 2012 and 2014 (Fig. 3b).

3.3. Inter annual variability in spatial occurrence of E. densa and water quality

Fig. 4 shows the variability in spatial occurrence of *E. densa*, as well as mean concentrations of TSS and mean water transparency across wetland sectors and years. Overall, the mean spatial occurrence of *E. densa* within the wetland increased through the study period, either in a linear fashion, or in a gradual sigmoid pattern (Table 3); on the other hand, the spatial occurrence of *E. densa* did not show any variation in sites located outside the wetland (Table 3, Fig. 4a). While all sectors across the wetland showed decreasing trends of TSS through time (Table 4, Fig. 4b); only sectors 4, 6 and 7 showed significant temporal trends ($p < 0.05$) (Table 4). Thus, sectors located along the central axis of the wetland (1, 2 and 3) did not show any significant temporal changes in TSS,

Table 2
Grading of histopathological alterations in livers of swans (counts) collected in the wetland during 2004–2005 ($n = 40$) and 2012 ($n = 13$). Autolysis or cell destruction in liver of swans collected during 2004–2005 precluded the analyses of histopathological characteristics with count lower than 40 individuals. Grades are: absence = 0; + = slight, ++ = mild, and +++ = severe (see Material and methods). Also compare with Fig. S1.

Histologic characteristics	Grading of histopathological alterations										Fisher's exact test
	2004–2005					2012					
	n	0	+	++	+++	*n*	0	+	++	+++	*P*-value
Hepatocytes positives to Prussian blue stain	40	0	2	14	24	13	2	8	2	1	0.0006
Hemosiderin deposits in Kupfer cells	38	0	17	18	3	13	3	10	0	0	0.0001
Periportal inflammation	40	0	10	26	4	13	1	9	3	0	0.0045
Perivascular fibrosis	40	8	15	14	3	13	13	0	0	0	0.0001
Proliferation of bile ducts	38	7	13	17	1	13	7	5	1	0	0.0221
Nuclear enlargement in hepatocytes	37	3	17	16	1	13	7	4	2	0	0.0049
Double nucleus in hepatocytes	37	5	23	9	0	13	9	4	0	0	0.0005
Necrosis in hepatocytes	37	16	17	4	0	13	12	1	0	0	0.0094

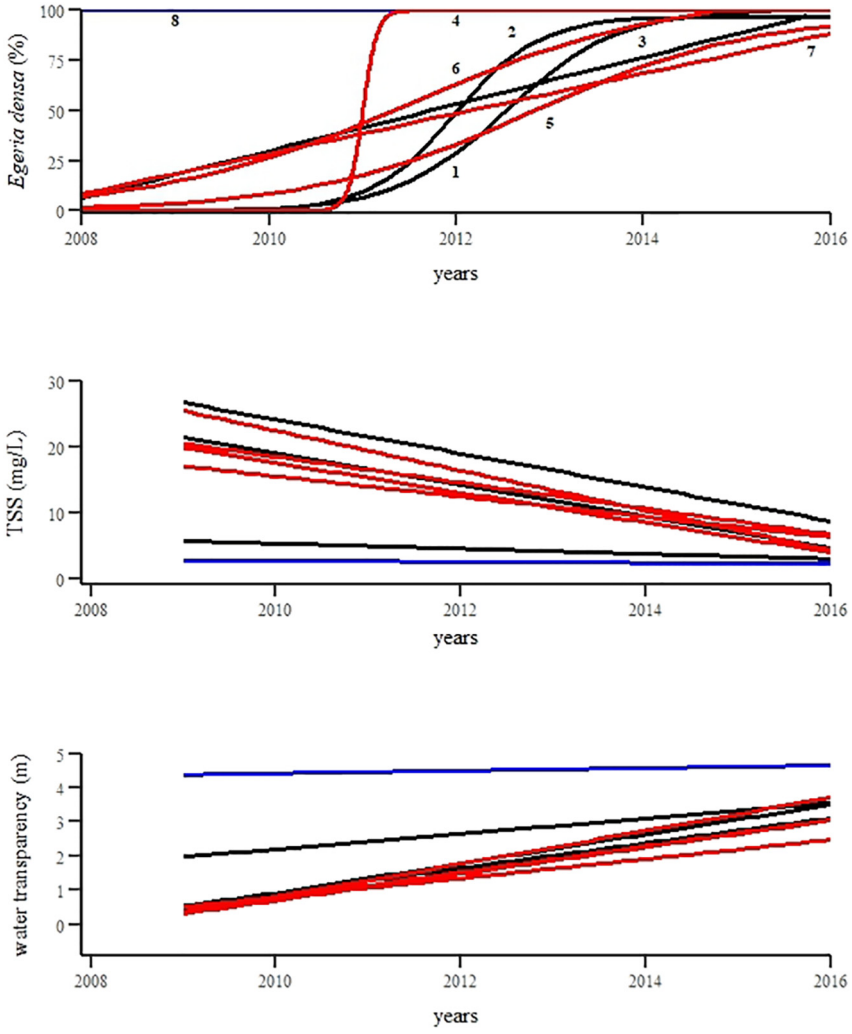

Fig. 4. Spatial occurrence (%) of *E. densa* (a), mean concentrations of Total Suspended Solids (TSS) (b) and water transparency (c) across sectors and years (cf. Fig. 1). Color of lines represent the different sectors studied across the wetland: black lines are for sectors located along the central axis of the wetland (1–3), red lines correspond to sectors located in tributaries (4–7), while blue lines correspond to the sites located outside the wetland (sector 8) (cf. Fig. 1). For the spatial occurrence of *E. densa*, model selection was carried out to choose between a logistic and linear model, while for TSS and water transparency, linear model functions are shown.

Table 3
Model selection for the spatial variation in the spatial occurrence of *E. densa* across the wetland during the study period. The table shows the fitted parameter values for the linear and sigmoid logistic models across studied sectors. The best model for each zone is highlighted in bold letters and with an asterisk. The coefficient of determination (R^2) and Bayesian Information Criterion (BIC) are also shown. The best model for each sector was shown by minimizing the BIC value and is highlighted in bold letters and asterisks.

Model	Sectors	Parameters			R^2	BIC
		a	b	c		
Linear	1	−29,621.25	14.74		0.64	209.99
Linear	2	−29,967.59	14.92		0.64	5.51E + 02
Linear	3	**−23,467.00**	**11.69**		**0.37**	**376.97***
Linear	4	−28,120.10	14.01		0.65	312.00
Linear	5	−26,287.52	13.09		0.48	258.58
Linear	6	−24,695.91	12.30		0.45	247.05
Linear	7	**−20,071.43**	**10.00**		**0.79**	**61.01***
Linear	8	−888.74	0.48		−0.17	5.43
Logistic	1	**100.53**	**1.69**	**2012.54**	**0.737**	**207.65***
Logistic	2	**97.29**	**2.08**	**2011.998**	**0.720**	**542.79***
Logistic	3	160.47	0.39	2014.72	0.394	380.05
Logistic	4	100.00	**13.16**	**2011.00**	**0.855**	**288.50***
Logistic	5	98.34	**0.84**	**2012.79**	**0.509**	**261.33***
Logistic	6	108.87	**0.73**	**2011.55**	**0.496**	**249.37***
Logistic	7	113.50	0.66	2012.50	0.857	84.85
Logistic	8	114.37	0.55	2011.57	0.044	8.30

Table 4
Linear model fitting for the spatial variation in TSS and water transparency across the wetland during the study period. The Table shows the fitted parameter values for the linear model, as well as the significance value for the model slope and the determination coefficient (R^2). Significant models are highlighted in bold and asterisks.

Variable	Sectors	Coefficients		*p* values	R^2
		a	b		
TSS	1	798.41	−0.39	0.437	0.12
TSS	2	4844.57	−2.40	0.055	0.55
TSS	3	5208.00	−2.58	0.288	0.22
TSS	**4**	**6129.74**	**−3.04**	**0.041**	**0.60***
TSS	5	3995.61	−1.98	0.195	0.31
TSS	**6**	**4598.40**	**−2.28**	**0.028**	**0.65***
TSS	**7**	**3126.00**	**−1.55**	**0.034**	**0.63***
TSS	8	177.50	−0.09	0.534	0.08
Water transparency	1	−448.03	0.22	0.061	0.62
Water transparency	2	−862.03	0.43	0.049	**0.66***
Water transparency	3	−733.40	0.37	0.050	**0.66***
Water transparency	**4**	**−779.17**	**0.39**	**0.024**	**0.76***
Water transparency	5	**−562.00**	**0.28**	**0.088**	**0.56**
Water transparency	**6**	**−972.03**	**0.48**	**0.030**	**0.73***
Water transparency	**7**	**−768.40**	**0.38**	**0.019**	**0.78***
Water transparency	8	−73.30	0.04	0.843	0.01

while those representing the tributaries Nanihue & Cudico (sector 4), Cayumapu (sector 6) and San Ramón (sector 7) presented significant trends towards decreasing values of TSS (Table 4). This suggests that the whole basin can be regarded as heterogeneous regarding the input of suspended particles, with tributary rivers to the wetland presenting improved levels of water quality throughout time, probably as a result of the input of fresh water with lower sediment loads. Water transparency showed some general significant improvements throughout the wetland, with sectors 1 and 5 (upper area of the wetland and Pichoy river, respectively) failing to show significant trends ($p > 0.05$) (Fig. 4c and Table 4). Thus, most sectors studied show clear trends towards improved water transparency throughout time. On the other hand, for the study sites located outside the wetland (i.e. sampling sites within sector 8), both TSS and water transparency did not show any significant temporal trend (Fig. 4c and Table 4). Hence, sites outside the wetland have not been impacted during the study period.

The above results are consistent with the observed inter-annual variability in HSI for *E. densa* within the wetland (Fig. 5). Spatial variation for this index in the spring-summer seasons of 1999–2000 was higher than that observed for the spring- summer season of 2004–2005 (Fig. 5). On the other hand, much higher values of HSI were estimated for the spring-summer periods of 2009–2010 and 2014–2015 (Fig. 5). Thus, the projected HSI values - based on the 2014–2015 data - are consistent with the recorded decrease of *E. densa* and its subsequent recovery within the wetland following the year 2004. Based on the observed HSI values, important spatial heterogeneity is detected across the northern and central areas of the wetland (Fig. 5). It is likely that observed spatial variation in HSI reflects local differences in river depth and water flow, as well as in TSS and water transparency (see Lagos et al., 2008). As an important caveat, it must be noted that competitive interactions with other aquatic plants may also determine empirical distribution of *E. densa* across the wetland, thus modifying the observed pattern in HSI. Further spatial field studies may provide additional information to describe and model the potential effects of biotic interactions on the spatial distribution and variability of this aquatic macrophyte in the wetland.

Changes in the spatial occurrence of *E. densa* may be also inferred from the interpretation of historical aerial imagery, collected during summer months at two areas of the upper reach of the Río Cruces wetland. Figs. 6 and 7 show the comparison of imagery collected in the years 1995, 2005, 2010 with a high-resolution (10 cm) drone photomosaic collected in 2016. The interpretation of *E. densa* stands in the drone

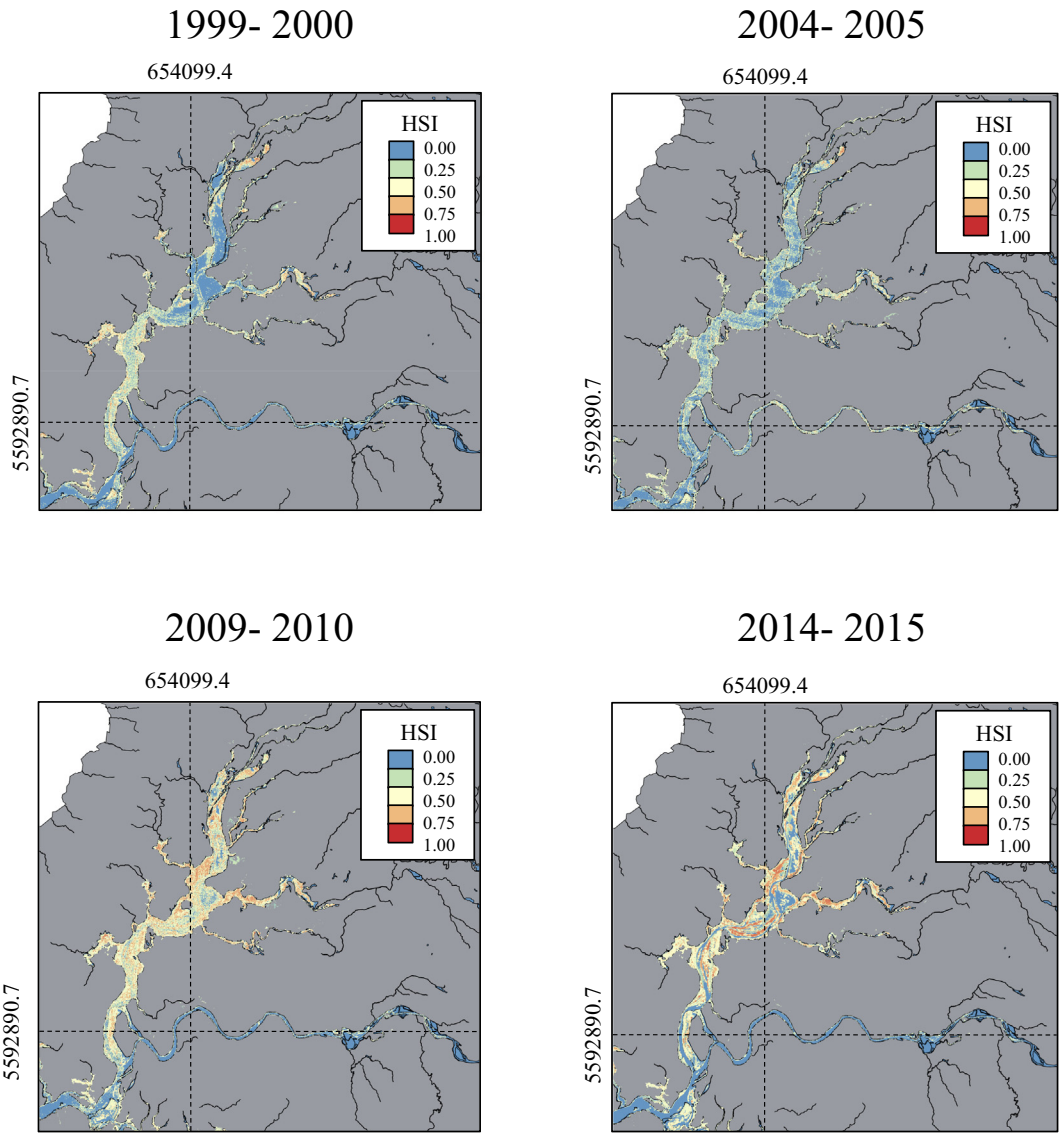

Fig. 5. Inter annual variability in habitat suitability index (HSI) for *E. densa* within the wetland. The figures show the spatial variation in HSI for the spring summer seasons of 1999–2000, 2004–2005, 2009–2010 and 2014–2015. The coordinates shown correspond to WSG84 UTM zone 18S.

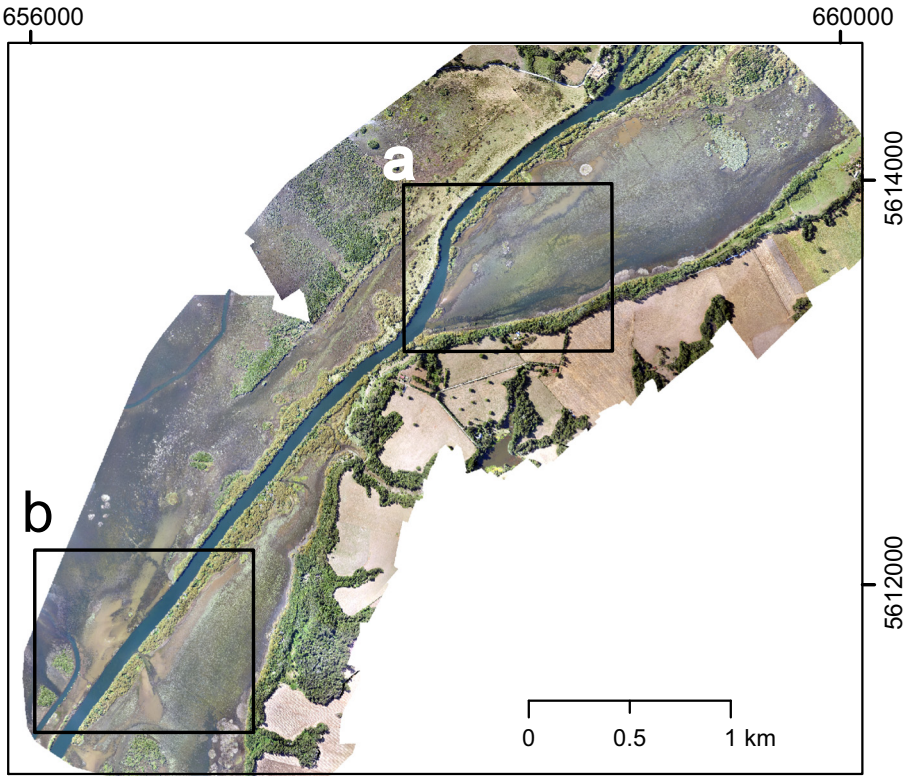

Fig. 6. Aerial photomosaic from the upper wetland area obtained with an Ebee drone in February 2016 (see Fig. 1 for location). Rectangles show locations of areas in Fig. 7.

image was based on field observations. The 1995 image shows abundant cover of plants in sedimentary tidal flats with discrete channels (Fig. 7); in turn, the images of 2005 and 2010 show that these channels had been covered by sediments without clear evidence of spatial occurrence of *E. densa*. The cover of tidal channels by sediments observed in historical aerial images in 2005 may be interpreted as a result of the decrease of *E. densa* (Escaida et al., 2014) and root detachment from the sedimentary substrate, causing extensive suspension of iron-rich sediments throughout the wetland. The channels visible in 1995 are again clearly distinguishable in the 2016 drone image, together with abundant plants (cf. Figs. 6 and 7).

Our results show that different hierarchical levels affected by a sudden short lived spillage from the pulp mill in 2004, recovered over time in a similar time scale. While the immediate mechanisms of this

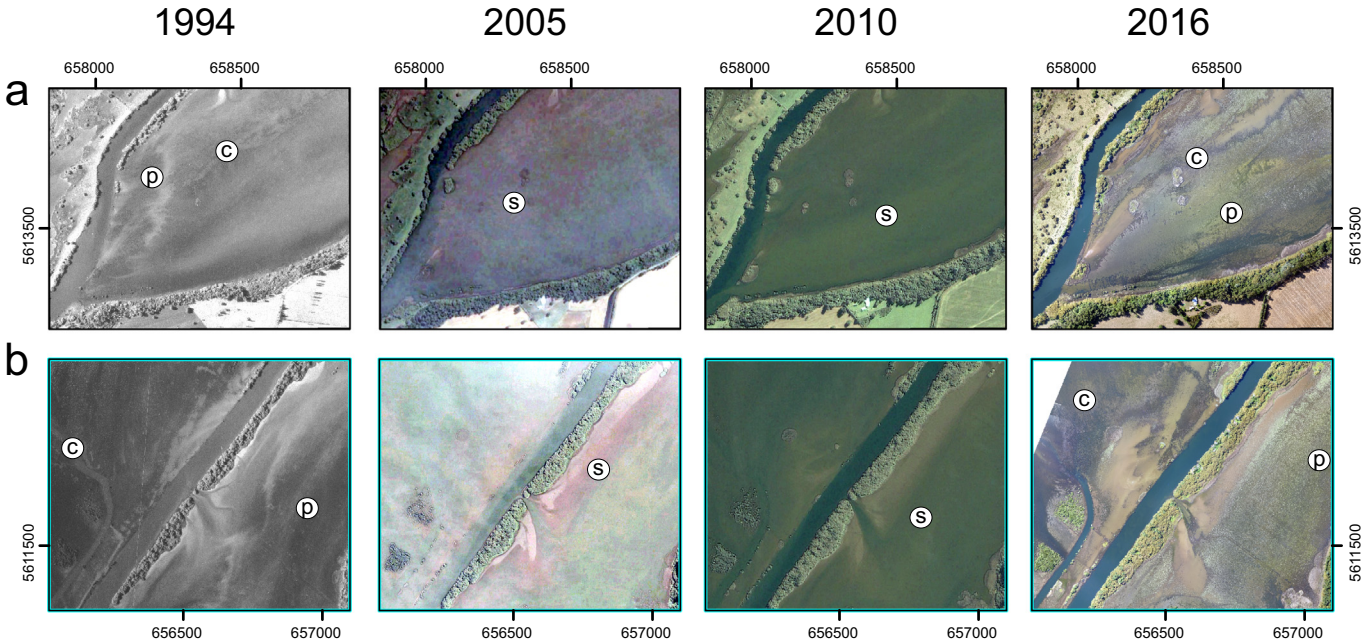

Fig. 7. Time series of aerial imaginary from the upper wetland (see Figs. 1 and 6 for location). c = shallow channels, p = plants of *E. densa*, s = sedimentary substrate devoid of plants. Note that the area covered by plants in 1995 was covered by sediments in 2005 (after the pulse disturbance event) and recovered back to plants between 2010 and 2016. Shallow channels visible in 1994 and 2016 were mostly filled by sediments in the 2005 images (see text for details).

disturbance differed across the components affected (i.e. *Egeria densa* and herbivorous water birds), the population recovery of *E. densa* seems to have governed the concomitant recovery of herbivorous swans. Thus, after the response to acute xenobiotic exposure, the ecosystem's response seems to have been modulated by the demographic response of the affected primary producer, highlighting the role of an ecosystem engineer placed at the base of the trophic chain. Furthermore, any other sudden disturbance impacting this species over a similar spatial and temporal extent would likely require similar recovery times (between 8 and 10 years). These could include disturbances which may not necessarily be anthropic in origin, such as volcanic ash deposits or alterations in the aquatic regime that may impact *E. densa*. On the other hand, either chronic or periodic exposures to pollution disturbance would likely result in different ecotoxicological responses and a less favorable scenario for ecosystem restoration efforts. In this regard, we have documented the ecosystem response of a wetland that is modulated by a dominant primary producer. Further studies are required to compare whether resilience times in ecosystems where autotrophic ecosystem engineers are like those in ecosystems where consumer's species have been affected.

4. Conclusions

Our surveys of the black necked swan population carried out from 1987 to 2016 in the Río Cruces wetland in southern Chile, shows different dynamic phases with inter and intra-annual fluctuations, interrupted by sudden environmental changes in 2004. After this event, swan population abundances, body weight and overall health conditions recovered in the following eight years back to pre-2004 states. This recovery phase was concomitant with changes in the spatial occurrence of *E. densa* as well as with the decrease of iron content in plant tissues and the improvement of water quality (i.e. decreased TSS and increased water transparency) across the wetland. The results of this study show the resilience capacity of important components of a temperate wetland after anthropogenic disturbances. These results have critical implications on the understanding of temporal scales over which conservation and management efforts in southern Chilean wetland ecosystems should be considered.

Supplementary data to this article can be found online at https://doi.org/10.1016/j.scitotenv.2018.01.333.

Acknowledgements

We are grateful to CONAF - Valdivia; especially to the rangers of the wetland Luis Miranda and Roberto Rosas for their assistance in the field and to Mario Maturana (the administrator of the wetland) for his enthusiastic support. This study was primarily supported by Comisión Nacional del Medio Ambiente (CONAMA, Chile) (grant number 1210-1203/2004-12-14), Servicio de Evaluación Ambiental (SEA, Chile) and Ministerio del Medio Ambiente (MMA, Chile). Partial financial support was provided by the Company ARAUCO during 2015 and 2016, under the research agreement with the Universidad Austral de Chile to carry out the environmental monitoring program of the wetland. We also acknowledge helpful comments made by two anonymous reviewers to a previous version of the manuscript.

References

Aarts, G., Fieberg, J., Matthiopoulos, J., 2012. Comparative interpretation of count, presence-absence and point methods for species distribution models. Methods Ecol. Evol. 3, 177–187.
Ahn, Y.H., Shanmugam, P., Ryu, J.H., 2004. Atmospheric correction of the Landsat satellite imagery for turbid waters. Gayana 68, 1–8.
Araya, B., Millie, G., 1986. Guía de Campo de las aves de Chile. 1ª ed. Editorial Universitaria, Santiago de Chile (389 pp).
Casares, J., 1933. Palmípedos Argentinos. Editorial El Homero. 5, pp. 145–159.
Chander, G., Markham, B., 2003. Revised Landsat-5 TM radiometric calibration procedures and post calibration dynamic ranges. IEEE Trans. Geosci. Remote Sens. 41, 2674–2677.
Cisternas, M., Atwater, B.F., Torrejón, F., Sawai, Y., Machuca, G., Lagos, M., Eipert, A., Youlton, C., et al., 2005. Predecessors of the giant 1960 Chile earthquake. Nature 437, 404–407.
Cork, S.C., 2000. Iron storage diseases in birds. Avian Pathol. 29, 7–12.
Corti, P., Schlatter, R., 2002. Feeding ecology of the Black necked swan *Cygnus melancoryphus* in two wetlands of southern Chile. Stud. Neotropical Fauna Environ. 37, 9–14.
Crawley, M.J., 2013. The R Book. First. Ed. John Wiley & Sons, New Delhi (975 pp).
Elith, J., Leathwick, J.R., 2009. Species distribution models: ecological explanation and prediction across space and time. Annu. Rev. Ecol. Evol. Syst. 40, 677–697.
Elith, J., Graham, C.H., Anderson, R.P., Dudik, M., Ferrier, S., Guisan, A., Hijmans, R.J., Huettmann, F., Leathwick, J.R., Lehmann, A., Li, J., Lohmann, L.G., Loiselle, B.A., Manion, G., Moritz, C., Nakamura, M., Nakazawa, Y., Overton, J.M., Peterson, A.T., Phillips, S.J., Richardson, K., Scachetti-Pereira, R., Schapire, R.E., Soberon, J., Williams, S., Wisz, M.S., Zimmermann, N.E., 2006. Novel methods improve prediction of species' distributions from occurrence data. Ecography 29, 129–151.
Elith, J., Phillips, S.J., Hastie, T., Dudík, M., Chee, Y.E., et al., 2011. A statistical explanation of MaxEnt for ecologists. Divers. Distrib. 11, 43–57.
Escaida, J., Jaramillo, E., Amtmann, C., Lagos, N., 2014. Crisis Socioambiental: el humedal del río Cruces y el Cisne de cuello negro. Ediciones UACh. Universidad Austral de Chile, Valdivia, Chile (260 pp).
Farina, L.L., Heard, D.J., LeBlanc, D.M., Hall, J.O., Stevens, G., Wellehan, J.F.X., Detrisac, C.J., 2005. Iron storage disease in captive Egyptian fruit bats (*Rousettus aegyptiacus*): relationship of blood iron parameters to hepatic iron concentrations and hepatic histopathology. J. Zoo. Wildl. Med. 36, 212–221.
Fisher, R.A., 1935. The Design of Experiments: Oliver & Boyd (Edinburgh).
Fithian, W., Hastie, T., 2013. Finite-sample equivalence in statistical models for presence-only data. Ann. Appl. Stat. 7, 1917–1939.
Frederick, P., Ogden, J., 2001. Pulsed breeding of long-legged wading birds and the importance of infrequent severe drought conditions in the Florida Everglades. Wetlands 21, 484–491.
Frederick, P., Gawlik, D.E., Ogden, J.C., Cook, M.I., Lusk, M., 2009. The white ibis and wood stork as indicators for restoration of the everglades ecosystem. Ecol. Indic. 9, S83–S95.
Gonzalez, A.L., Fariña, J.M., 2013. Changes in the abundance and distribution of black-necked swans (*Cygnus melancoryphus*) in the Carlos Anwandter Nature Sanctuary and Adjacent Wetlands, Valdivia, Chile. Waterbirds 36, 507–514.
Gosselin, S.J., Kramer, L.W., 1983. Pathophysiology of excessive iron storage in mynah birds. J. Am. Vet. Med. Assoc. 183, 1238–1240.
Ives, A.R., 1995. Measuring resilience in stochastic systems. Ecol. Monogr. 65, 217–233.
Jaramillo, E., Schlatter, R., Contreras, H., Duarte, C., Lagos, N., Paredes, E., Ulloa, J., Valenzuela, G., Peruzzo, B., Silva, R., 2007. Emigration and mortality of Black-necked swans (*Cygnus melancoryphus*) and disappearance of the macrophyte *Egeria densa* in a Ramsar wetland site of southern Chile. Ambio 36, 607–609.
Jaramillo, E., Duarte, C., Labra, F., Lagos, N., Peruzzo, B., Silva, R., Velasquez, C., Manzano, M., Melnick, D., 2017. Temporal Scales of Resilience of an Aquatic Macrophyte Exposed to an Anthropogenic-induded Environmental Stressor in a Ramsar Wetland of Southern Chile (Submitted to Ambio).
Jaramillo, E., Duarte, C., Labra, F., Lagos, N., Peruzzo, B., Silva, R., Velasquez, C., Manzano, M., Melnick, D., 2018. Resilience of an aquatic macrophyte exposed to an anthropogenic-induced environmental stressor in a Ramsar wetland of southern Chile. Ambio. (in review).
Kincaid, A.L., Stoskopf, M.K., 1987. Passerine dietary iron overload syndrome. Zoo Biology 6, 79–88.
Klasing, K.C., Dierenfeld, E.S., Koutsos, E.A., 2012. Avian iron storage disease: variations on a common theme? J. Zoo Wildl. Med. 43, 27–34.
Klopfleisch, R., Olias, P., 2012. The pathology of comparative animal models of human haemochromatosis. J. Comp. Pathol. 147, 460–478.
Lagos, N.A., Paolini, P., Jaramillo, E., Lovengreen, Ch., Duarte, C., Contreras, H., 2008. Environmental processes, water quality degradation, and decline of waterbird populations in the Río Cruces wetland, Chile. Wetlands 28, 938–950.
Lee, Z., Shang, S., Qi, L., Yan, J., Lin, G., 2016. A semi-analytical scheme to estimate Secchi-disk depth from Landsat-8 measurements. Remote Sens. Environ. 177, 101–106.
Lowenstine, L.J., Munson, L., 1999. Iron overload in the animal kingdom. In: Fowler, M.E., Miller, R.E. (Eds.), Zoo and Wild Animal Medicine: Current Therapy 4. PA, Saunders, Philadelphia, pp. 260–268.
Lowenstine, L.J., Stasiak, I.M., 2015. Update on iron overload in zoologic species. Fowler's Zoo and Wild Animal Medicine, 8va ed. Elsiever, Saunders, Missouri, pp. 674–681.
Masek, J.G., Vermote, E.F., Saleous, N., Wolfe, R., Hall, F.G., Huemmrich, F., Gao, F., Kutler, J., Lim, T.K., 2006. A Landsat surface reflectance data set for North America, 1990–100. IEEE Geosci. Remote Sens. Lett. 3, 68–72.
McIntyre, C., 2015. Changes in the abundance and distribution of trumpeter swans in Denali. Alaska Park Sci. 5, 25–29.
Mete, A., Dorrestein, G.M., Marx, J.J.M., Lemmens, A.G., Beynen, A.C., 2001. A comparative study of iron retention in mynahs, doves and rats. Avian Pathol. 30, 479–486.
Mete, A., Hendriks, H.G., Klaren, P.H.M., Dorrestein, G.M., van Dijk, J.E., Marx, J.J.M., 2003. Iron metabolism in mynah birds (*Gracula religiosa*) resembles human hereditary haemochromatosis. Avian Pathol. 32, 625–632.
Miller-Ihli, N.J., 1990. Slurry sampling for graphite furnace atomic absorption spectrometry. Anal. Bioanal. Chem. 337, 271–274.
Naeem, S., Li, S., 1997. Biodiversity enhances ecosystem reliability. Nature 390, 507–509.
Navas, J., 1977. Aves Anseriformes. In: Ringuelet, A.A. (Ed.), Fauna de Agua Dulce de la República Argentina. Fecic, Buenos Aires. 43, pp. 1–94.
Neubert, M.G., Caswell, H., 1997. Alternatives to resilience for measuring the responses of ecological systems to perturbations. Ecology 78, 653–665.
Ortega-Huerta, M.A., Peterson, A.T., 2008. Modeling ecological niches and predicting geographic distributions: a test of six presence-only methods. Rev. Mex. Biodivers. 79, 205–216.

Papes, M., Gaubert, P., 2007. Modelling ecological niches from low numbers of occurrences: assessment of the conservation status of poorly known viverrids (Mammalia, Carnivora) across two continents. Divers. Distrib. 13, 890–902.
Pearson, R.G., Raxworthy, C.J., Nakamura, M., Peterson, A.T., 2007. Predicting species distributions from small numbers of occurrence records: a test case using cryptic geckos in Madagascar. J. Biogeogr. 34, 102–117.
Phillips, S.J., Dudík, M., 2008. Modeling of species distributions with Maxent: new extensions and a comprehensive evaluation. Ecography 31, 161–175.
Phillips, S.J., Dudík, M., Schapire, R.E., 2004. Un enfoque de máxima entropía para modelar la distribución de especies. En Actas de la XXI Conferencia Internacional Sobre Aprendizaje Automático. ACM, p. 83.
Phillips, S.J., Anderson, R.P., Schapire, R.E., 2006. Maximum entropy modeling of species geographic distributions. Ecol. Model. 190, 231–259.
Pinochet, D., Ramírez, C., MacDonald, R., Riedel, L., 2004. Concentraciones de elementos minerales en *Egeria densa* Planch. colectada en el Santuario de la Naturaleza Carlos Anwandter, Valdivia, Chile. Agro Sur 32, 80–86.
Plafker, G., Savage, J.C., 1970. Mechanism of the Chilean earthquakes of May 21 and 22, 1960. Geol. Soc. Am. Bull. 81, 1001–1030.
R Development Core Team, 2014. R: A Language and Environment for Statistical Computing. 2014. R Foundation for Statistical Computing, Vienna URL. http://www.R-project.org.
Ramírez, C., San Martín, C., Medina, R., Contreras, D., 1991. Estudio de la Flora Hidrófila del Santuario de la Naturaleza "Río Cruces" (Valdivia, Chile). Gayana Bot. 48, 67–80.
Ramírez, C., Carrasco, E., Mariani, S., Palacios, N., 2006. La desaparición del Luchecillo (*Egeria densa*) del Santuario del Río Cruces (Valdivia, Chile): Una Hipótesis plausible. Ciencia y Trabajo. 8, pp. 79–86.
Renner, I.W., Warton, D.I., 2013. Equivalence of MAXENT and Poisson point process models for species distribution modelling in ecology. Biometrics 69, 274–281.
San Martín, C., Contreras, D., Ramírez, C., 2000. El recurso vegetal del Santuario de la Naturaleza Carlos Anwandter (Valdivia, Chile). Rev. Geogr. Valpso. 31, 225–235.
Saville, D.J., 1990. Multiple comparison procedures: the practical solution. Am. Stat. 44, 174–180.
Schlatter, R., 1998. El Cisne de Cuello Negro (*Cygnus melanocoryphus*) en Chile. In: Valverde, V. (Ed.), La Conservación de la Fauna Nativa de Chile, Logros y Perspectivas. CONAF, Ministerio de Agricultura, Chile, pp. 121–131.
Schlatter, R., Salazar, J., Villa, A., Meza, J., 1991a. Demography of black-necked swans *Cygnus melancoryphus* at three Chilean wetland areas. In: Sears, J., Bacon, P. (Eds.), Proceedings Third IWRB International Swan Symposium. Wildfowl, Suppl. 1 1989. Oxford, pp. 88–94.
Schlatter, R., Salazar, J., Villa, A., Meza, J., 1991b. Reproductive Biology of Black-necked Swans *Cygnus melancoryphus* at three Chilean Wetland Areas and Feeding Ecology at Río Cruces. Wildfowl, Suppl. 1 pp. 268–271.
Schlatter, R.P., Navarro, R.O., Corti, P., 2002. Effects of El Niño southern oscillation on numbers of black-necked swans at río Cruces Sanctuary, Chile. Colon. Waterbirds 25 (Special Publication 1), 114–122.
Schwarz, G., 1978. Estimating the dimension of a model. Ann. Stat. 6, 461–464.
Silva, C.P., Schlatter, R.P., Soto-Gamboa, M., 2012. Reproductive biology and pair behavior during incubation of the black-necked swan (*Cygnus melanocoryphus*). Ornitol. Neotrop. 23, 555–567.
Skagen, S.K., Adams, A.A.Y., 2012. Weather effects on avian breeding performance and implications of climate change. Ecol. Appl. 22, 1131–1145.
Snell-Rood, E.C., Cristol, D.A., 2003. Avian communities of created and natural wetlands: bottomland forests in Virginia. Condor 105, 303–315.
Sokal, R., Rohlf, F., 1995. Biometry the Principles and Practice of Statistics in Biological Research. W.H. Freeman, New York.
Steubing, L., Ramírez, C., Alberdi, M., 1980. Energy content of water and bog plant associations in the region of Valdivia (Chile). Vegetatio 43, 153–161.
Strickland, J.D.H., Parsons, T.R., 1972. A Practical Handbook of Seawater Analysis. Bulletin No. 157. second edition. Fisheries Research Board of Canada, Ottawa, Canada (310 pp).
Timpane-Padgham, B.L., Beechie, T., Klinger, T., 2017. A systematic review of ecological attributes that confer resilience to climate change in environmental restoration. PLoS ONE 12 (3), e0173812. https://doi.org/10.1371/journal.pone.0173812.
Travsky, A., Beauvais, G.P., 2004. Species Assessment for the Trumpeter Swan (*Cygnus buccinator*) in Wyoming. United States Department of the Interior Bureau of Land Management, Wyoming State Office, Cheyenne, Wyoming (29 pp).
Trexel, J., Travis, J., 1993. Nontraditional regression analyses. Ecology 74, 1629–1637.
UACh (Universidad Austral de Chile), 2005. Informe Final "Estudio sobre origen de mortalidades y disminución poblacional de aves acuáticas en el Santuario de la Naturaleza Carlos Anwandter, en la Provincia de Valdivia". Convenio UACh-CONAMA (443 pp).
UACh (Universidad Austral de Chile), 2014. Informe Final: Diagnóstico Ambiental del Humedal del río Cruces basado en la comparación de condiciones ambientales actuales e históricas: Bases para su monitoreo y sustentabilidad. Convenio UACh-MMA (374 pp).
UACh (Universidad Austral de Chile), 2015. Programa de Diagnóstico Ambiental del Humedal del Río Cruces y sus Ríos Tributarios (1508 pp).
UACh (Universidad Austral de Chile), 2017. Programa de Monitoreo Ambiental Actualizado del Humedal del Río Cruces y sus Ríos Tributarios (830 pp).
Verdugo, C., 2004. Valores Hematológicos del Cisne de Cuello Negro (*Cygnus melanocoryphus*, Molina 1782) en una Población Silvestre, Valdivia, Chile. (Tesis Escuela de Medicina Veterinaria). Universidad Austral de Chile, Valdivia, Chile, p. 54.
Vilina, Y.A., Cofre, H.L., Silva-Garcia, C., Garcia, M.F., Perez-Friedenthal, C., 2002. Effects of El Niño on abundance and breeding of Black-necked swans on El Yali wetland in Chile. Waterbirds 25, 123–127.
Walker, B., Holling, C.S., Carpenter, S.R., Kinzig, A., 2004. Resilience, adaptability and transformability in social-ecological systems. Ecol. Soc. 9 (5) [online] URL:. http://www.ecologyandsociety.org/vol9/iss2/art5/.
Wand, M.P., Jones, M.C., 1995. Kernel Smoothing. Chapman and Hall, London.
Wand, M., Ripley, B., 2015. Functions for Kernel Smoothing Supporting Wand & Jones (1995). R Package Version 2. 23-15.
Ward, R.J., Lancu, T.C., Henderson, G.M., Kirkwood, J.K., Peters, T.J., 1988. Hepatic iron overload in avian species: analytical and morphological studies. Avian Pathol. 17, 451–464.
Wisz, M.S., Hijmans, R.J., Li, J., Peterson, A.T., Graham, C.H., Guisan, A., 2008. NCEAS predicting species distributions working group. Effects of sample size on the performance of species distribution models. Divers. Distrib. 14, 763–773.
Woelfl, S., Mages, M., Encina, F., Bravo, F., 2006. Trace metals in microcrustaceans and brazilian waterweed from a contaminated Chilean wetland using total reflection X-ray fluorescence spectrometry. Microchim. Acta 154, 261–268.
Xu, H., 2006. Modification of normalized difference water index (NDWI) to enhance open water features in remotely sensed imagery. Int. J. Remote Sens. 27:3025–3033. https://doi.org/10.1080/01431160600589179.
Zar, J.H., 1999. Biostatistical Analysis. Fourth Edition. Prentice-Hall, Upper Saddle River, New Jersey.
Zedler, J.B., Kercher, S., 2005. Wetland resources: status, trends, ecosystem services, and restorability. Annu. Rev. Environ. Resour. 30, 39–74.